

Effects of Toroidally Distributed Divertor Biasing on Scrape-Off-Layer Plasma in the QUEST Spherical Tokamak^{*})

Kazuo TOI, Takumi ONCHI¹⁾, Kengo KURODA¹⁾, Shinichiro KOJIMA¹⁾, Hideki ZUSHI¹⁾, Makoto HASEGAWA¹⁾, Masaharu FUKUYAMA¹⁾, Shoji KAWASAKI¹⁾, Aki HIGASHIJIMA¹⁾, Tatsuya IKEZOE¹⁾, Hiroshi IDEI¹⁾, Takeshi IDO¹⁾, Kazuaki HANADA¹⁾ and QUEST Experiment Group¹⁾

National Institute for Fusion Science, Toki 509-5292, Japan

¹⁾*Research Institute for Applied Mechanics, Kyusyu University, Kasuga 816-8580, Japan*

(Received 18 November 2020 / Accepted 7 January 2021)

A novel divertor biasing using four biasing plates that are arranged toroidally every 90° on the upper divertor plate is applied to low-density plasmas of the QUEST spherical tokamak. When some of these plates are biased in-phase by applying a sawtooth waveform voltage of 85-V amplitude and 50-Hz repetition, up to approximately 35% reduction of the particle flux to the divertor is observed during positive biasing. The input power for the flux reduction is approximately 0.2 kW for low-density tokamak plasmas produced by ~130-kW electron cyclotron wave injection. Additionally, the signal of a plate probe placed in the low-field side of the mid-plane of the vacuum vessel indicates enhanced losses of fast electrons during positive biasing. The enhanced loss is attributed to small resonant magnetic perturbations produced by the bias-driven currents in the scrape-off layer. This novel divertor biasing is expected to provide a new experimental tool for studying divertor heat load control and fast electron confinement in a tokamak device.

© 2021 The Japan Society of Plasma Science and Nuclear Fusion Research

Keywords: scrape-off layer (SOL), divertor heat load, divertor biasing, radial transport in SOL, SOL current, resonant magnetic perturbation

DOI: 10.1585/pfr.16.2402024

1. Introduction

In a future large fusion device, the large heat load to divertor should be controlled to avoid serious damage to divertor targets. A candidate scenario is a detached divertor operation, which introduces impurity gases to the divertor region. The main concern is that the detached divertor operation may degrade the pedestal performance of H-mode plasma. Maintaining good H-mode confinement over a longer time scale is challenging because the detached divertor operation tends to increase upstream density, which leads to the degradation of the H-mode confinement. Although various experiments are being attempted to maintain good H-mode confinement in the detached divertor operation, good H-mode confinement with the improvement factor $H_{98y} \sim 1$ is sustained for a relatively short time scale, thus far, on the order of several seconds [1]. In ASDEX-Upgrade, a partially detached divertor can achieve both low divertor heat load and good H-mode confinement through a careful feedback control of impurity feeding into the divertor region [2]. However, after the transition to pronounced detachment by a small excess of neutral pressure and injected impurities, the H_{98y} index is reduced to a level less than unity (~ 0.7) [2]. The

compatibility of divertor heat load control and high core plasma confinement in detached divertor operation will be more severe in next-generation devices such as the International Thermonuclear Experimental Reactor (ITER) and the DEMONstration toroidal fusion power plant (DEMO). New control methods of divertor heat load for relaxing the requirements for injected impurities in the detached divertor operation are required to avoid undesirable confinement degradation. Thus, developing new advanced divertor configurations is a viable approach [3–5]. Another approach is to explore the possibility of enhanced radial particle and heat transport in the scrape-off layer (SOL), the enhanced transport of which would broaden the divertor heat load profile and decrease the heat load on the targets. The idea of a toroidally non-axisymmetric divertor concept is an interesting proposal [6, 7]; it was tested in the MAST spherical tokamak [8]. This paper presents the initial results of the toroidally-distributed-divertor-biasing experiment on the QUEST spherical tokamak.

2. Experimental Setup

Four biasing plates are toroidally arranged every 90° on the upper divertor plate, which comprises 16 fan-shaped segments, as shown in Fig. 1 (a). The short and long toroidal widths of the stainless biasing plate with a trapezoidal shape are 0.15 and 0.19 m, respectively. One of

author's e-mail: toi.kazuo@toki-fs.jp

^{*}) This article is based on the presentation at the 29th International Toki Conference on Plasma and Fusion Research (ITC29).

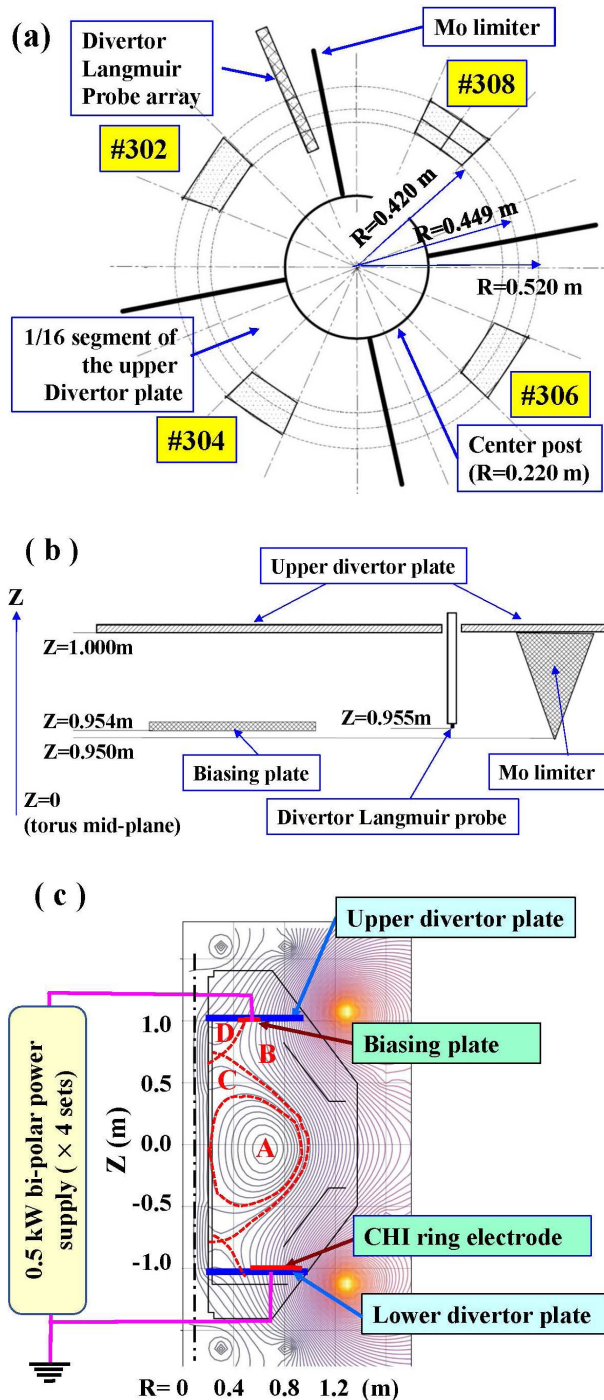


Fig. 1 (a) Four biasing plates #302 to #308 toroidally arranged on the upper divertor plate. One of the biasing plates, #308, is divided into four pieces with a 2 mm gap. The divertor Langmuir-probe (DLP) array and four molybdenum (Mo-) limiters are paced on the upper divertor plate. (b) Vertical arrangement of the biasing plate, DLP, and Mo-limiter. (c) Biasing electrical circuit for each biasing plate consists of a bi-polar power supply and the CHI (coaxial helicity injection) ring electrode. The poloidal flux surfaces of a typical target plasma for the divertor biasing are also shown.

the biasing plates, #308, is divided into four pieces with a 2 mm gap to study leak currents from the biased flux tube. The front surface of the biasing plate is adjusted to the vertical position $Z = 0.954$ m, which is 4 mm behind the molybdenum (Mo-) limiter at $Z = 0.950$ m, where the mid-plane of the torus is at $Z = 0$ m (Fig. 1 (b)). Note that the horizontal locations of these components are not scaled in real size. The high-field side mouth and the right and left sides of each biasing plate are covered with alumina insulator plates to avoid the loss of bias-driven currents to the vacuum vessel via tenuous plasma in the rear side of the biasing plate.

Each biasing plate is connected to a respective bi-polar power supply, as shown in Fig. 1 (c). The maximum output voltage and current are 100 V and 5 A, respectively. Various voltage waveforms, such as sawtooth up to 20 kHz repetition, generated by a function generator are amplified by the bipolar power supply. In this experiment, sawtooth waveform voltage of 85 V and 50 Hz repetition is applied to each biasing plate. Each biasing plate can be biased in-phase or out-of-phase relative to other biasing plates. The phasing between four plates can specify the toroidal mode number n of the applied potential pattern as $n = 0, 1, 2,$ and 4 . In Fig. 1 (c), the magnetic configuration of target plasma for the biasing experiment is also shown, where the toroidal magnetic field is ~ 0.25 T at the magnetic axis ($R \sim 0.65$ m). The target plasma is limited by the inboard side, because the magnetic separatrix of the high-field side unexpectedly intersects with the guard limiter tiles on the center post of the tokamak, as shown in Fig. 1 (c). Thus, the tokamak core plasma (marked “A”) is surrounded by “inner” SOL (marked “C”), which is defined by the guard limiter on the center post, and “inner” SOL is further surrounded by “outer” SOL (marked “B”), which is defined by the low-field-side magnetic separatrix. This configuration has two X-points; therefore, “outer” SOL has a character of double-null configuration. In this configuration, we can study the responses of SOL and divertor plasmas via divertor biasing. Hereafter, we call “outer” SOL simply “SOL”. Depending on the position of outer and upper divertor legs that intersect with the biasing plate, the biasing can also drive currents in the private region (marked “D”) of the upper divertor as well as the SOL. An appreciable amount of bias-driven currents is detected by a full toroidal ring electrode for the co-axial helicity injection (CHI) experiment [9] on the lower divertor plate, where the electrode is grounded using a 1- Ω resistor for current detection.

3. Experimental Results

Figure 2(a) shows the time evolution of toroidal plasma current (I_p) and line-integrated electron density ($n_e L$) of a typical target plasma for divertor biasing. The line-averaged electron density is $\sim 1 \times 10^{18} \text{ m}^{-3}$ at $t \sim 2.6$ s. The sum of currents driven by three biasing plates of the

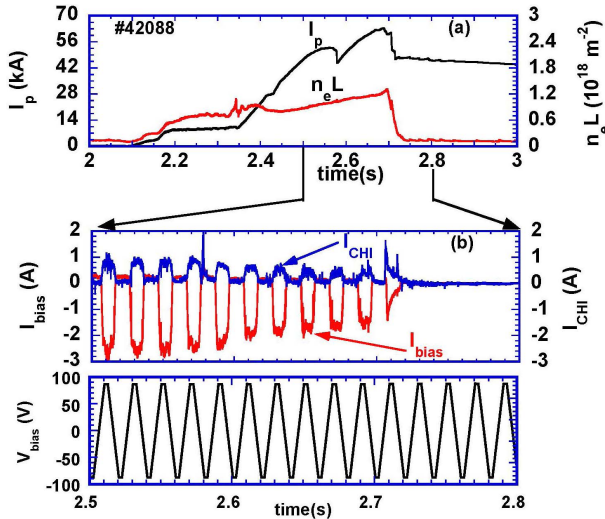


Fig. 2 (a) Waveforms of plasma current (I_p) and line integrated electron density ($n_e L$) of a typical target plasma for the divertor biasing, where the plasma is pre-ionized by 8.2 GHz electron cyclotron heating (ECH) from $t = 1.8$ s to 2.4 s, and the plasma current is ramped up by 28 GHz ECH of ~ 130 kW from $t = 2.1$ –2.7 s. (b) Total current driven by three biased plates (I_{bias}), current detected by the CHI electrode (I_{CHI}), and biasing voltage. The positive sign of I_{bias} and I_{CHI} stands for the current that flows into the plate or electrode.

same shape (#302, #304, and #306) (I_{bias}) and the current detected by the CHI electrode (I_{CHI}) are shown in Fig. 2 (b) together with the biasing voltage waveform. The current I_{bias} gradually decreases with a slow increase in $n_e L$ in the high I_p phase. The inverse response of I_{bias} for $n_e L$ indicates that the core confinement improvement by increased line-averaged electron density in the higher I_p phase decreases the SOL electron density. The logarithmic value of I_{bias} for the applied voltage V_{bias} may provide information on electron temperature in front of the biased plate, i.e., $T_{e,bp} \sim 10$ eV. The radial decay length of electron density (λ_{SOL}) in SOL at the outer mid-plane is crudely estimated as $\lambda_{SOL} \sim 2.7$ cm, assuming the electron temperature at the mid-plane $T_{e,omp} (= 4T_{e,bp}) = 40$ eV and ion temperature $T_{i,omp} = 2T_{e,omp}$. Considering the ion saturation current of ~ 0.17 A at $t = 2.65$ s, the electron density averaged over λ_{SOL} in front of the biased plate is estimated as $n_{e,bp} \sim 3 \times 10^{16} \text{ m}^{-3}$.

Figure 2 (b) shows that current I_{CHI} is approximately 30% of I_{bias} during positive biasing, whereas extracting the negative biasing effect from I_{CHI} is difficult because of a slowly varying positive component that exists in a shot without biasing. The magnitude of I_{bias} during positive biasing is larger than that during negative biasing by a factor of ~ 12 . The length of magnetic flux tube affected by biasing may be estimated by “the large electrostatic probe” model, as $L_{||ef} = hd^2 v_{the} / [8(d+h)D_n]$ in collisionless SOL plasma approximation for electron

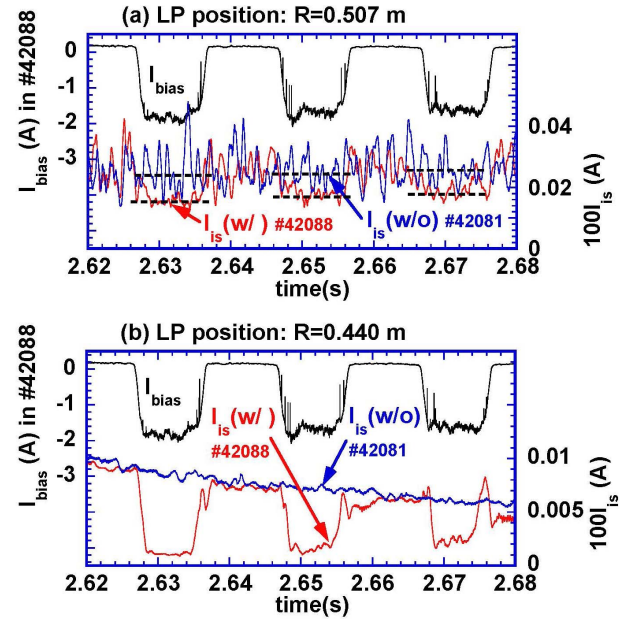


Fig. 3 Comparison of the ion saturation currents I_{is} at (a) $R = 0.507$ m and (b) $R = 0.440$ m in the upper divertor region for two shots with (#42088) and without (#42081) the biasing, together with I_{bias} . The measurement positions $R = 0.507$ m and 0.440 m correspond to the SOL and the private region, respectively. The signals I_{is} are averaged for every 0.5 ms time-window.

flow [10, 11], where h , d , v_{the} , and D_n are the projection width of the plate to the SOL magnetic field line, radial decay length of density, electron thermal velocity, and particle diffusion coefficient, respectively. Assuming that $T_e = (T_{e,bp} + T_{e,omp})/2$ and $D_n = D_{Bhom}/3$, using $d = \lambda_{SOL} \sim 0.027$ m and plausible parameters, $L_{||ef} \sim 25$ m is obtained and is comparable with the connection length of SOL, $L_c \sim 2\pi R q_{SOL} \sim 21$ m with $q_{SOL} \sim 4$ and $\bar{R} \sim 0.83$ m. The mean free path of electrons in SOL is $\lambda_e \sim 270$ m, assuming $n_e = (n_{e,bp} + n_{e,omp})/2$ and $n_{e,omp} = n_{e,bp}/4$. Even under the condition of $\lambda_e \gg L_{||ef} \gtrsim L_c$, the SOL current driven by positive biasing is much larger than the ion saturation current at the grounded end plate. The interpretation of the observation of the SOL-current flow channel is too complex and is a future research subject.

Figure 3 shows the time evolution of ion saturation currents I_{is} measured by a divertor Langmuir probe array at two radial positions $R = 0.507$ m and 0.440 m in the high plasma current phase, together with I_{bias} , where negative I_{bias} is driven by positive biasing and indicates the current flowing out of the biased plate. The divertor flux I_{is} at $R = 0.440$ m rapidly starts decreasing from $t = 2.58$ s and decreases to $\sim 1/7$ of the value at $t = 2.5$ s, where large low-frequency fluctuations in I_{is} are suppressed. This result indicates that the divertor leg is on the upper and outboard side, i.e., the strike point moves outward in time during the slow ramp-up of I_p . Thus, the monitoring position of Langmuir probe $R = 0.440$ m moves from the “outer”

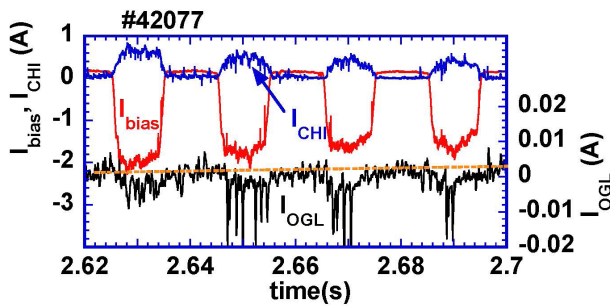


Fig. 4 Time evolution of particle loss flux I_{OGL} measured in the outer mid plane, by a plate probe grounded with a 1- Ω resistor, together with the bias-drive current I_{bias} and the CHI electrode detected current I_{CHI} . Negative signal of I_{OGL} indicates the flow-in of electrons to the probe. The horizontal broken line indicates the level without the biasing.

SOL to the private region. Conversely, the Langmuir probe placed at $R = 0.507$ m remains in the SOL throughout the high I_p phase. In this shot, three plates of the same shape are biased in-phase with a sawtooth voltage of 85 V. Figure 3(a) shows that the divertor flux at $R = 0.507$ m is reduced by approximately 30% - 35% during positive biasing compared with that without biasing, whereas clear changes in the flux are not observed during negative biasing. The total input power by biasing is ~ 150 W for positive biasing and ~ 17 W for negative biasing. The reduced divertor flux will be transported to the outboard-side wall of the torus. However, the divertor fluxes measured by additional outside Langmuir probes from $R = 0.537$ m to $R = 0.725$ m behave in a complex way. Specifically, the fluxes from $R = 0.537$ m to $R = 0.597$ m do not show clear changes, but decrease by approximately 20% - 40% at both $R = 0.627$ m and $R = 0.657$ m. The fluxes at $R = 0.687$ m and beyond the position do not show any changes. The effect of biasing on the private region is stronger, as shown in Fig. 3(b). The reduced flux will be directed to the upper and inboard leg area. The present arrangement of the divertor biasing system and target plasma condition may result in complex responses in the divertor flux. The reduction rate of divertor flux changes depending on the number of biased plates, i.e., $\sim 20\%$ by one plate biasing and $\sim 25\%$ by two neighboring plates, respectively. In this experiment, the phase of applied biasing voltage between the plates is set to be in-phase to determine the conversion rate of I_{bias} to the SOL current. The operation of out-of-phase neighboring two biasing plates is expected to lead to a more pronounced reduction in divertor flux because a large potential difference will be produced toroidally [6].

The magnetic flux tube is strongly deformed because of a strong magnetic shear near the upper and lower X-points [12]. The potential perturbations by biasing may not extend beyond the upper X-point toward the outer-mid plane of a plasm because of the shear effect, as theoreti-

cally predicted by [6], the character of which may impede the generation of SOL-current filaments reaching the unbiased lower divertor plate. However, negative disturbances in the I_{OGL} signal are clearly observed during negative I_{bias} driven by positive biasing, as shown in Fig. 4. Here the loss current I_{OGL} is detected by a grounded plate probe installed on the outer mid-plane of the vacuum vessel. The negative disturbance indicates the enhanced losses of fast electrons produced by electron cyclotron waves. Small resonant magnetic perturbations produced by several SOL-current filaments [13] are thought to be a possible cause of the losses.

4. Summary and Outlook

A novel divertor biasing has been tested in the QUEST. The observed decrease in divertor flux is interpreted to be induced by the toroidally non-axisymmetric divertor action, which enhances the outward convection flux in SOL. Moreover, the divertor biasing enhances fast electron losses to the outer mid-plane region. This observation indicates the effects of resonant magnetic perturbations produced by bias-driven SOL currents. The divertor biasing is a powerful tool for studying interactions among SOL, divertor plasma, and the edge of core plasma. The optimized arrangement of biasing plates and the fine tuning of phasing and amplitude of applied voltage to the plates are needed to maximize the biasing effect.

Acknowledgments

One of the authors (K. T.) would like to acknowledge Prof. S. Ohdachi (NIFS), Prof. S. Masuzaki (NIFS), and Dr. S. Yamamoto (QST) for their support in the initial phase of this research. This research is supported in part by a Grant-in-Aid for Scientific Research from JSPS (No. 26630476) and by NIFS under NIFS18KUTR133.

- [1] A.R. Field *et al.*, Plasma Phys. Control. Fusion **59**, 095003 (2017).
- [2] A. Kallenbach *et al.*, Nucl. Fusion **55**, 053026 (2015).
- [3] D.D. Ryutov, Phys. Plasmas **14**, 064502 (2007).
- [4] M. Kotschenreuther *et al.*, Phys. Plasmas **14**, 072502 (2007).
- [5] P.M. Valanju *et al.*, Phys. Plasmas **16**, 056110 (2009).
- [6] R.H. Cohen and D.D. Ryutov, Nucl. Fusion **37**, 621 (1997).
- [7] D.D. Rutov, P. Helander and R.H. Cohen, Plasma Phys. Control. Fusion **43**, 1399 (2001).
- [8] C. F. Counsell *et al.*, Nucl. Fusion **43**, 1197 (2003).
- [9] K. Kuroda *et al.*, Plasma Phys. Control. Fusion **60**, 115001 (2018).
- [10] S.A. Cohen *et al.*, J. Nucl. Mater. **76&77**, 68 (1978).
- [11] P.C. Stangeby, J. Phys. D: Appl. Phys. **18**, 1547 (1985).
- [12] D. Farina, R. Pozzoli and D.D. Ryutov, Nucl. Fusion **33**, 1315 (1993).
- [13] I. Joseph, R.H. Cohen and D.D. Ryutov, Phys. Plasmas **16**, 052510 (2009).